

Draft genomes of a male and female Australian jacky dragon (*Amphibolurus muricatus*)

Ran Tian^{1,2,‡}, Hao Dong^{1,‡}, Fan Zhang¹, Hao Yu¹, Enqing Pei¹, Chengcheng Shi^{3,4}, Guangyi Fan^{3,4}, Sarah L. Whiteley^{5,6}, Clare E. Holleley⁶, Inge Seim^{1,7}, Arthur Georges^{5,8*}

¹ Integrative Biology Laboratory, College of Life Sciences, Nanjing Normal University, Nanjing 210046, China

² Jiangsu Key Laboratory for Biodiversity and Biotechnology, College of Life Sciences, Nanjing Normal University, Nanjing 210046, China

³ BGI-Qingdao, Qingdao 266555, China

⁴ BGI-Shenzhen, Shenzhen 518083, China

⁵ Institute for Applied Ecology, University of Canberra ACT 2617, Australia

⁶ Australian National Wildlife Collection, CSIRO, Canberra ACT 2601, Australia

⁷ School of Biology and Environmental Science, Queensland University of Technology, Brisbane Qld 4000, Australia

⁸ AusARG consortium, Bioplatforms Australia, Macquarie University NSW 2109, Australia

* Corresponding author: Institute for Applied Ecology, University of Canberra, ACT 2601, Australia. E-mail: georges@aerg.canberra.edu.au

‡These authors contributed equally to this work and share first authorship.

1 **ABSTRACT**

2 Australia is remarkable for its lizard diversity, with very high endemism because of
3 continental-scale diversification and adaptive radiation during prolonged isolation. We
4 employed stLFR linked-read technology to generate male and female draft genomes of the
5 jacky dragon *Amphibolurus muricatus*, an Australian dragon lizard (family Agamidae). The
6 assemblies are 1.8 Gb in size and have a repeat content (39%) and GC content (42%) similar
7 to that of other dragon lizards. The longest scaffold was 39.7 Mb (female) and 9.6 Mb (male),
8 with corresponding scaffold N50 values of 6.8 Mb and 1.6 Mb. The BUSCO (Sauropsida
9 database) completeness percentages were 90.2% and 88.8% respectively. These statistics are
10 comparable to those for other lizard genomes. Phylogenetic comparisons show that
11 Australian dragon lizard species split from a common ancestor about 35.4 million years ago.
12 The draft *A. muricatus* assemblies will be a valuable resource for understanding lizard sex
13 determination and the evolution and conservation of Australian dragon lizards.

14

15 **Keywords:** agamid lizard; Agamidae; squamate; nuclear genome; genome assembly

16

17

18

19

20 **Introduction**

21 The Australian jacky dragon *Amphibolurus muricatus* (**Figure 1**) is a lizard that is
22 widespread in dry sclerophyll forests of south-eastern and eastern Australia (Cogger 2014). It
23 is a model species for biogeography (Pepper et al. 2014), evolutionary biology (Warner et al.
24 2013; Warner and Shine 2008), social behaviour (Peters and Evans 2003; Woo and Rieucau
25 2013) and development (Whiteley et al. 2021; Esquerré et al. 2014).

26 Species in the genus *Amphibolurus* and *Chlamydosaurus* are a major clade in the
27 Australian radiation of the Agamidae (Hugall et al. 2008). The draft assembly of *A.*
28 *muricatus*, together with that of *Pogona vitticeps* (Georges et al. 2015), represents the first
29 foray into generating the necessary high-quality genomes for the Agamidae. In particular,
30 *A. muricatus* occupies mesic habitats and so is intermediate between the Australian water
31 dragon *Intellagama lesueurii* and the forest dragon *Lophosaurus boydii* that occupy hydric
32 habitats, and the central bearded dragon *Pogona vitticeps* and the Lake Eyre dragon
33 *Ctenophorus maculosus*, for example, that occupy more xeric habitats. As such, it is one of
34 several species important for understanding genomic adaptation to the progressive aridity that
35 has occurred in Australia in the past 15 Myr. *Amphibolurus muricatus* is also of particular
36 interest because it has temperature-dependent sex determination (TSD) (Harlow and Taylor
37 2000) and it is unclear as to whether this arises from classical TSD or a combination of
38 genetic and environmental influences (Whiteley et al. 2021). Studies of the underlying
39 mechanisms of TSD require a genome assembly and knowledge of genome organisation to
40 identify genes on the sex chromosomes of species with genotypic sex determination (GSD)
41 and their chromosomal and gene homology in closely related TSD species. This is
42 particularly so in species with TSD that show evidence of cryptic residual or de novo
43 genotypic influence on offspring sex ratios, as is suspected for *A. muricatus* (Whiteley et al.
44 2021).

45 Here, we generated draft, annotated genome assemblies for a male and a female *A.*
46 *muricatus* that are comparable in contiguity and completeness to other published agamid
47 genomes. We used transcriptomes sequenced and assembled for *A. muricatus* and published
48 assemblies (*Anolis*, *Varanus* and *Pogona*) to annotate the genomes. Our assemblies will
49 provide a resource to increase capacity and accelerate the progress of studies into the
50 evolution, ecology, and conservation of Australian dragon lizards.

51

52

53

54 **Materials and methods**

55

56 **Sample collection**

57 To reduce the high heterozygosity that presented difficulties in the assembly of the genome of
58 *Pogona vitticeps* (Georges et al., 2015), we generated inbred lines of *A. muricatus*. The
59 founding male and female pair were sourced from the wild and bred in captivity. The two
60 animals used to generate the genome were obtained from the fourth generation of the inbred
61 pedigree produced by sib-sib matings and back crossing (see **Figure S1** for the complete
62 pedigree). The male (AA069033) and female (AA069032) individuals used for the genome
63 and transcriptome sequencing were humanely euthanised via intraperitoneal injection of
64 sodium pentobarbitone (60 mg/ml in isotonic saline). Organs were rapidly dissected and snap
65 frozen in liquid nitrogen.

66

67 **DNA extraction**

68 High molecular weight DNA was extracted from liver (female) and blood (male). DNA yield
69 and quality was assessed using a NanoDrop spectrophotometer (Thermo Fisher Scientific,
70 Waltham, MA, USA) and a Qubit fluorometer (Thermo Fisher Scientific) and pulse-field gel
71 electrophoresis.

72

73 **Assembly 1.0: A 10x Genomics linked-read sequencing assembly**

74 Male and female *A. muricatus* genome sequencing libraries were constructed on the
75 Chromium system (10x Genomics, Pleasanton, CA, USA) by the Ramaciotti Centre for
76 Genomics (Sydney, Australia). The Chromium instrument enables unique barcoding of long
77 stretches of DNA on gel beads. The barcodes allow later reconstruction of long DNA
78 fragments from a series of short DNA fragments with the same barcode (i.e., linked-reads).
79 After barcoding, DNA was sheared into smaller fragments and sequenced on the NovaSeq
80 6000 platform (Illumina, CA, USA) to generate 151 bp paired-end (PE) reads. A total of
81 904.9 M raw 10x Genomics Chromium linked-reads were generated. Raw 10x data were
82 assembled with Supernova v2.1.1 (Weisenfeld et al. 2017) and a FASTA file was generated
83 using the ‘pseudohap style’ option in Supernova mkoutput. All female (~450 M) and male
84 (~550 M) read pairs were used (female sequencing depth *ca* 50.3×; male, *ca* 47.8×). The
85 resulting assemblies were further scaffolded with ARKS v1.0.3 (Coombe et al. 2018), reusing
86 the 10x reads and the companion LINKS program (v1.8.7) (Warren et al. 2015). ARKS
87 employs a *k*-mer approach to map linked barcodes to the contigs in the initial Supernova

88 assembly to generate a scaffold graph with estimated distances for LINKS input. These
89 assemblies were denoted AmpMurF_1.0 (female) and AmpMurM_1.0 (male). We used
90 GapCloser v1.12 (part of SOAPdenovo2) (Luo et al. 2012) to fill gaps in the assembly.
91 GapCloser was run using the parameter -l 150) and clean 10x Genomics reads PE reads.
92

93 **Assembly 1.1: Further scaffolding of assembly 1.0 using RNA-seq data**

94 We attempted to improve the v1.0 genome assemblies' contiguity using RNA-sequencing
95 reads. RNA-seq reads (from brain, ovary, and testis; see below) were filtered (i.e., cleaned) to
96 remove adapters and low-quality reads using Flexbar v3.4.0 and used to further re-scaffold
97 the v1.0 assemblies (FASTA files before gapclosing) with P_RNA_scaffolder (Zhu et al.
98 2018). The default Flexbar settings discards all reads with any uncalled bases. A final round
99 of scaffolding was performed on the resulting assemblies using L_RNA_scaffolder (Xue et
100 al. 2013). These assemblies were denoted AmpMurF_1.1 (female) and AmpMurM_1.1
101 (male). As before, GapCloser and clean 10x Genomics reads were used to fill gaps.
102

103 **Assembly 2.0: Further scaffolding of assembly 1.0 using SLR-superscaffolder**

104 As an alternative approach, we attempted to improve the v1.0 genome assemblies' contiguity
105 using SLR-superscaffolder (Guo et al. 2021). Briefly, SLR-superscaffolder employs single
106 tube long fragment read (stLFR) sequencing (Wang et al. 2019) reads (see section below) to
107 generate hybrid genome assemblies. The software was run with default parameters except for
108 PE_SEED_MIN=300 (minimum contig size to fill; default 1000). These assemblies were
109 denoted AmpMurF_2.0 (female) and AmpMurM_2.0 (male). GapCloser and clean stLFR
110 reads (with the barcode removed using https://github.com/BGI-Qingdao/stLFR_barcode_split) were used to fill gaps.
111

113 **Assembly 3.0: An stLFR linked-read sequencing assembly**

114 We also generated independent assemblies for the individuals sequenced on the 10x
115 Genomics Chromium system using single tube long fragment read (stLFR) sequencing
116 (Wang et al., 2019). BGI (Brisbane, Australia) generated ~100× coverage 100-bp paired-end
117 reads (plus a 42-bp stLFR barcode on the right/_2 read) per individual. Low-quality reads,
118 PCR duplicates, and adaptors were removed using SOAPnuke v1.5 (Chen et al. 2018). All
119 female (~1,517 M) and male (~1,427 M) read pairs were utilised. The stLFRdenovo pipeline
120 (<https://github.com/BGI-biotools/stLFRdenovo>), which is based on Supernova v2.11 and

121 customised for stLFR data, was used to generate a *de novo* genome assembly. The
122 stLFRdenovo tool ‘FillGaps’ was used to fill gaps.
123

124 **RNA-seq and transcriptome assembly**

125 Raw data 125 bp PE reads, generated on an Illumina HiSeq 2500 instrument was filtered
126 using Flexbar v3.4.0 (Roehr et al. 2017; Dodt et al. 2012) with default settings (eliminates
127 reads with any uncalled bases). Any residual ribosomal RNA reads (the majority removed by
128 poly(A) selection prior to sequencing library generation) were removed using SortMeRNA
129 v2.1b (Kopylova et al. 2012) against the SILVA v119 ribosomal database (Quast et al. 2013).
130 Tissue transcriptomes were de novo assembled using Trinity v2.11.0 (Haas et al. 2013;
131 Grabherr et al. 2011; Henschel et al. 2012) and assessed using BUSCO.
132

133 **Genome annotation**

134 We identified repetitive elements by integrating homology and *de novo* prediction data.
135 Protein-coding genes were annotated using homology-based prediction, *de novo* prediction,
136 and RNA-seq-assisted prediction methods.

137 Homology-based transposable elements (TE) annotations were obtained by
138 interrogating a genome assembly with known repeats in the Repbase database v16.02 (Bao et
139 al. 2015) using RepeatMasker v4.0.5 (DNA-level) (Tarailo-Graovac and Chen 2009) and
140 RepeatProteinMask (protein-level; implemented in RepeatMasker). *De novo* TE predictions
141 were obtained using RepeatModeler v1.1.0.4 (Smit and Hubley 2010) and LTRharvest v1.5.8
142 (Ellinghaus et al. 2008) to generate database for a RepeatMasker run. Tandem Repeat Finder
143 (v4.07) (Benson 1999) was used to find tandem repeats (TRs) in the genome. A non-
144 redundant repeat annotation set was obtained by combining the above data.

145 Protein-coding genes were annotated using homology-based prediction, *de novo*
146 prediction, and RNA-seq-assisted [generated from ovary, testis, and brain (both sexes)]
147 prediction methods. Sequences of homologous proteins from three lizards [*Anolis*
148 *carolinensis* (green anole) assembly AnoCar2.0 (RefSeq assembly GCF_000090745.1)
149 (Alfoldi et al. 2011); *Varanus komodoensis* (Komodo dragon) assembly ASM479886v1
150 (GCA_004798865.1) (Lind et al. 2019); and *Pogona vitticeps* (central bearded dragon)
151 assembly pvi1.1 (GCF_900067755.1)] (Georges et al. 2015) were downloaded from NCBI.
152 These protein sequences were aligned to the repeat-masked genome using BLAT v0.36 (Kent
153 2002). GeneWise v2.4.1 (Birney et al. 2004) was employed to generate gene structures based
154 on the alignments of proteins to a genome assembly. *De novo* gene prediction was performed

155 using AUGUSTUS v3.2.3 (Stanke et al. 2006), GENSCAN v1.0 (Burge and Karlin 1997),
156 and GlimmerHMM v3.0.1 (Majoros et al. 2004) with a human training set. Transcriptome
157 data (clean reads) were mapped to the assembled genome using HISAT2 v2.1.0 (Kim et al.
158 2019) and SAMtools v1.9 (Li et al. 2009), and coding regions were predicted using
159 TransDecoder v5.5.0 (Grabherr et al. 2011; Haas et al. 2013). A final non-redundant
160 reference gene set was generated by merging the three annotated gene sets using
161 EvidenceModeler v1.1.1 (EVM) (Haas et al. 2008) and excluding EVM gene models with
162 only ab initio support. The gene models were translated into amino acid sequences and used
163 in local BLASTp (Camacho et al. 2009) searches against the public databases Kyoto
164 Encyclopedia of Genes and Genomes (KEGG; v89.1) (Kanehisa and Goto 2000), NCBI non-
165 redundant protein sequences (NR; v20170924) (O'Leary et al. 2016), Swiss-Prot (release-
166 2018_07) (UniProt Consortium 2012), and InterPro (v69.0) (Mitchell et al. 2019).
167

168 **Phylogeny and divergence time estimation**

169 In addition to *A. carolinensis*, *V. komodoensis* and *P. vitticeps* (see section above), the
170 genome and sequences of homologous proteins from *Gekko japonicus* (Schlegel's Japanese
171 gecko) assembly *Gekko_japonicus_V1.1* (GCA_001447785.1) (Liu et al. 2015) and *Crotalus*
172 *tigris* (tiger rattlesnake) assembly *ASM1654583v1* (GCA_016545835.1) (Margres et al.
173 2021) were downloaded from NCBI. The genome and annotations of *Ophisaurus gracilis*
174 (Anguidae lizard) were downloaded from GigaDB (Song et al. 2015a; Song et al. 2015b). No
175 gene annotation data were available for three species: *Intellagama lesueuri* (Australian water
176 dragon; assembly *EWD_hifiasm_HiC* generated as part of the AusARG consortium and
177 (downloaded from DNA Zoo (Dudchenko et al. 2018; Cheng et al. 2021; Dudchenko et al.
178 2017)) and the Chinese agamid lizards *Phrynocephalus przewalskii* (Przewalski's toadhead
179 agama) (Gao et al. 2019) and *Phrynocephalus vlangalii* (Ching Hai toadhead agama) (Gao et
180 al. 2019) (CNCBdb accession no. CNP0000203). Their protein-coding genes were annotated
181 using homology-based prediction, de novo prediction, and RNA-seq-assisted prediction
182 methods (see genome annotation section above).

183 We identified 4,441 high-confidence 1:1 orthologs by interrogating the predicted
184 proteins from the gene models of ten species using SonicParanoid v1.3.0 (Cosentino and
185 Iwasaki 2019). The corresponding coding sequences (CDS) for each species were aligned
186 using PRANK v100802 (Loytynoja and Goldman 2005) and filtered by Gblocks v0.91b
187 (Talavera and Castresana 2007) to identify conserved blocks (removing gaps, ambiguous
188 sites, and excluding alignments less than 300 bp in size), leaving 4,441 genes. Maximum-

189 likelihood (ML) phylogenetic trees were generated using RaxML v7.2.8 (Stamatakis 2006)
190 and IQ-Tree v2.1.3 (Minh et al. 2020) with three CDS data sets: the whole coding sequence
191 (whole-CDS), first codon positions, and fourfold degenerate (4d) sites. Identical topologies
192 and similar support values were obtained (1,000 bootstrap iterations were performed). The
193 divergence time between species was estimated using MCMCTree [a Bayesian molecular
194 clock model implemented in PAML v4.7 (Yang 2007)] with the JC69 nucleotide substitution
195 model, and the whole-CDS ML tree and concatenated whole-CDS supergenes as inputs. We
196 used 100,000 iterations after a burn-in of 10,000 iterations. MCMCTree calibration points
197 (million years ago; Mya) were obtained from (Oliver and Hugall 2017) (crown age of
198 Australian agamids 27.1 Mya, with 95% CI 20.1-37.7) and TimeTree (Kumar et al. 2017): *G.*
199 *japonicus*-*P. przewalskii* (190-206 Mya), *V. komodoensis*-*O. gracilis* (121-143 Mya), *V.*
200 *komodoensis*-*C. tigris* (156-174 Mya), *V. komodoensis*-*A. carolinensis* (155-175 Mya), *I.*
201 *lesueurii*-*A. carolinensis* (139-166 Mya), *I. lesueurii*-*P. przewalskii* (73-93 Mya), *I. lesueurii*-
202 *A. muricatus* (25.5-42.4 Mya), *P. vitticeps*-*A. muricatus* (20.2-34.6 Mya).

203 **Results and discussion**

204

205 **Draft genome assembly and comparisons with other squamates**

206 The genome-wide heterozygosity of our inbred *A. muricatus* lines was estimated (from stLFR
207 data) to range from 0.66% (female) to 0.73% (male), slightly lower than the central bearded
208 dragon (*Pogona vitticeps*) (0.85%) (Georges et al. 2015). We generated four genome
209 assemblies per sample. The v1.0 assemblies were generated using 10x Genomics Chromium
210 data and the Supernova assembler and further refined using ARKS and LINKS. The v1.1
211 assemblies employed P_RNA_scaffolder (uses RNA-seq reads from brain, ovary, and testis)
212 (**Table S1**) and L_RNA_scaffolder (uses Trinity transcriptome assemblies) (**Tables S2** and
213 **S3**) to improve the v1.0 assemblies, while the v2.0 assemblies used SLR-superscaffolder and
214 stLFR reads to improve the v1.0 assemblies. Finally, the 3.0 assemblies were generated using
215 stLFR reads alone and Supernova. While re-scaffolding of the assemblies generated using
216 10x Genomics Chromium sequencing improved the initial v1.0 assembly (in particular, SLR-
217 superscaffolder), assembly using stLFR data alone gave the best assembly result (**Table 1**).
218 The final, v3.0 assemblies have a total scaffold length (i.e., containing gaps) of ~1.8 Gb. The
219 longest scaffold was 39.7 Mb (female; AmpMurF_3.0) and 9.6 Mb (male; AmpMurM_3.0),
220 and the corresponding scaffold N50 values of 6.9 and 1.6 Mb. The contig N50s were 67.2 kb
221 (AmpMurF_3.0) and 59.3 kb (AmpMurM_3.0). The N50 values are similar to those of other
222 squamate genome assemblies (**Figure 2**), except for the chromosome-assigned assemblies of
223 Australian water dragon (*Intellagama lesueuri*; scaffold N50 268.9 Mb and contig N50 11.2
224 Mb), tiger rattlesnake (*Crotalus tigris*; scaffold and contig N50 2.1 Mb) (Margres et al.
225 2021), green anole (*Anolis carolinensis*; scaffold N50 150.1 Mb and contig N50 79.9 kb), and
226 Komodo dragon (*Varanus komodoensis*; scaffold N50 23.8 Mb and contig N50 189.3 kb)
227 (Lind et al. 2019).

228 The BUSCO metrics of the *A. muricatus* assemblies also compare well to other
229 squamate assemblies, including agamids from Australia [*P. vitticeps* (Georges et al. 2015)
230 and *I. lesueuri* (Australian water dragon)] and China (toad-headed agamas of genus
231 *Phrynocephalus* sp. (Gao et al. 2019)) (**Figure 3**) and **Table S5**).

232

233 **Genome annotation**

234 The *A. muricatus* assemblies are composed of ~38% repeat elements and have a GC content
235 of ~42% (**Tables S4 and S6**), similar to that of *P. vitticeps* (Georges et al. 2015) – with
236 LINEs being the predominant subtype. Protein-coding genes were annotated by combining

237 transcriptome evidence with homology-based (*A. carolinensis*, *V. komodoensis*, and *P.*
238 *vitticeps*) and de novo gene prediction methods. Gene statistics (**Table S8**) (see (Georges et
239 al. 2015)) and gene set BUSCO scores (**Table S9**) are comparable to other squamates. Using
240 ab initio, transcriptome, and homology-based prediction methods, we functionally annotated
241 21,655 (95.12%) and 21,799 (94.70%) protein-coding genes in the female and male assembly
242 (**Tables S10 and S11**) and recovered 89.2% and 88.2% of 7,480 sauropsid (i.e., non-avian
243 reptiles and birds) benchmarking universal single-copy orthologs (BUSCOs), respectively.

244
245 **Phylogenetic relationships**

246 To construct a time-calibrated species tree (**Figure 4**), we identified 4,441 high-confidence
247 single-copy orthologs from the female *A. muricatus* assembly and nine other squamate
248 species. There are currently five agamid lizard genome assemblies: three Australian dragon
249 lizard assemblies (*A. muricatus*, *P. vitticeps*, and *I. lesueuri*) and two toad-headed agama
250 assemblies (genus *Phrynocephalus*) (Gao et al. 2019; Georges et al. 2015). Our analysis
251 shows that the five agamid species shared an ancestor about 78.0 Mya [72.6-88.4 Mya 95%
252 credibility interval (CI)]. We estimate that the three Australian dragon lizard species split
253 from a common ancestor about 35.4 Mya (95% CI 31.5-38.4), while the lineages leading to
254 *A. muricatus* and *P. vitticeps* diverged 26.7 Mya (95% CI 20.6-31.0). These observations
255 agree with previous dating from a small set of genes and fossil data (Hugall et al. 2008;
256 Oliver and Hugall 2017).

257
258 **Conclusions and perspectives**

259 In this study, we generated the first annotated genome assemblies of *Amphibolurus*
260 *muricatus*. Overall, the assemblies are similar in quality to a range of squamate genomes and
261 will be immediately useful for the understanding of agamid lizard evolution, ecology, and
262 conservation.

263 **Data availability**

264 *A. muricatus* raw 10x Genomics genome and transcriptome sequencing reads have been
265 deposited to the NCBI Short Read Database (BioProject ID: PRJNA767251). Raw stLFR
266 genome sequencing reads have been deposited at the China National GeneBank Nucleotide
267 Sequence Archive (CNSA: <https://db.cngb.org/cnsa>) under accession number CNP0004768.
268 The male and female *A. muricatus* assemblies are available at Zenodo (Tian et al. 2023a).
269 Gene annotation files and associated FASTA files for *A. muricatus* (assembly AmpMurF_3.0
270 and AmpMurM_3.0), *I. lesueurii*, *P. przewalskii*, and *P. vlangalii* are available at Zenodo
271 (Tian et al. 2023b). *A. muricatus* transcriptome assemblies are available at Zenodo (Tian et al.
272 2021). Various scripts used for data processing and analyses are available on GitHub at
273 <https://github.com/sciseim/JackyDragon>.

274

275 **Acknowledgements**

276 We thank Dr Wendy Ruscoe and Jacqui Richardson for their assistance in generating the
277 inbred line of *A. muricatus* and for animal husbandry.

278

279 **Conflict of interest**

280 The authors declare there is no conflict of interest.

281

282 **Ethics Approvals**

283 All sampling and breeding experiments were conducted with approval of the Animal Ethics
284 Committee of the University of Canberra and in accordance with their Standard Operating
285 Procedures.

286

287 **Funding**

288 Financial support for this work was provided by an Australian Research Council Discovery
289 Grant (DP170101147; to A.G. and C.E.H.), a specially-appointed Professor of Jiangsu
290 Province grant (to I.S.), the Jiangsu Science and Technology Agency (to I.S.), the Jiangsu
291 Foreign Expert Bureau (to I.S.), the Jiangsu Provincial Department of Technology (grant
292 JSSCTD202142 to I.S.), the National Natural Science Foundation of China (grant 32270441
293 to R.T.), the National Key Programme of Research and Development, Ministry of Science
294 and Technology (grant 2022YFF1301601 to R.T.), and a 2023-2025 China Association for
295 Science and Technology Young Talent project (to R.T.).

296

297 **Literature cited**

298 Alfoldi, J., F. Di Palma, M. Grabherr, C. Williams, L. Kong *et al.*, 2011 The genome of the
299 green anole lizard and a comparative analysis with birds and mammals. *Nature* 477
300 (7366):587-591.

301 Bao, W., K.K. Kojima, and O. Kohany, 2015 Repbase Update, a database of repetitive
302 elements in eukaryotic genomes. *Mob DNA* 6:11.

303 Benson, G., 1999 Tandem repeats finder: a program to analyze DNA sequences. *Nucleic
304 Acids Res* 27 (2):573-580.

305 Birney, E., M. Clamp, and R. Durbin, 2004 GeneWise and Genomewise. *Genome Res* 14
306 (5):988-995.

307 Burge, C., and S. Karlin, 1997 Prediction of complete gene structures in human genomic
308 DNA. *J Mol Biol* 268 (1):78-94.

309 Camacho, C., G. Coulouris, V. Avagyan, N. Ma, J. Papadopoulos *et al.*, 2009 BLAST+:
310 architecture and applications. *BMC Bioinformatics* 10:421.

311 Chen, Y., Y. Chen, C. Shi, Z. Huang, Y. Zhang *et al.*, 2018 SOAPnuke: a MapReduce
312 acceleration-supported software for integrated quality control and preprocessing of
313 high-throughput sequencing data. *Gigascience* 7 (1):1-6.

314 Cheng, H., G.T. Concepcion, X. Feng, H. Zhang, and H. Li, 2021 Haplotype-resolved de
315 novo assembly using phased assembly graphs with hifiasm. *Nat Methods* 18 (2):170-
316 175.

317 Cogger, H., 2014 *Reptiles and amphibians of Australia*: CSIRO publishing.

318 Coombe, L., J. Zhang, B.P. Vandervalk, J. Chu, S.D. Jackman *et al.*, 2018 ARKS:
319 chromosome-scale scaffolding of human genome drafts with linked read kmers. *BMC
320 Bioinformatics* 19 (1):234.

321 Cosentino, S., and W. Iwasaki, 2019 SonicParanoid: fast, accurate and easy orthology
322 inference. *Bioinformatics* 35 (1):149-151.

323 Dodt, M., J.T. Roehr, R. Ahmed, and C. Dieterich, 2012 FLEXBAR-Flexible Barcode and
324 Adapter Processing for Next-Generation Sequencing Platforms. *Biology (Basel)* 1
325 (3):895-905.

326 Dudchenko, O., S.S. Batra, A.D. Omer, S.K. Nyquist, M. Hoeger *et al.*, 2017 De novo
327 assembly of the Aedes aegypti genome using Hi-C yields chromosome-length
328 scaffolds. *Science* 356 (6333):92-95.

329 Dudchenko, O., M.S. Shamim, S.S. Batra, N.C. Durand, N.T. Musial *et al.*, 2018 The
330 Juicebox Assembly Tools module facilitates de novo assembly of mammalian
331 genomes with chromosome-length scaffolds for under \$1000. *BioRxiv*:254797.

332 Ellinghaus, D., S. Kurtz, and U. Willhoeft, 2008 LTRharvest, an efficient and flexible
333 software for de novo detection of LTR retrotransposons. *BMC Bioinformatics* 9:18.

334 Esquerré, D., J.S. Keogh, and L.E. Schwanz, 2014 Direct effects of incubation temperature
335 on morphology, thermoregulatory behaviour and locomotor performance in jacky
336 dragons (*Amphibolurus muricatus*). *Journal of Thermal Biology* 43:33-39.

337 Gao, W., Y.B. Sun, W.W. Zhou, Z.J. Xiong, L. Chen *et al.*, 2019 Genomic and
338 transcriptomic investigations of the evolutionary transition from oviparity to
339 viviparity. *Proc Natl Acad Sci U S A* 116 (9):3646-3655.

340 Georges, A., Q. Li, J. Lian, D. O'Meally, J. Deakin *et al.*, 2015 High-coverage sequencing
341 and annotated assembly of the genome of the Australian dragon lizard *Pogona
342 vitticeps*. *Gigascience* 4:45.

343 Grabherr, M.G., B.J. Haas, M. Yassour, J.Z. Levin, D.A. Thompson *et al.*, 2011 Full-length
344 transcriptome assembly from RNA-Seq data without a reference genome. *Nat
345 Biotechnol* 29 (7):644-652.

346 Guo, L., M. Xu, W. Wang, S. Gu, X. Zhao *et al.*, 2021 SLR-superscaffolder: a de novo
347 scaffolding tool for synthetic long reads using a top-to-bottom scheme. *BMC
348 Bioinformatics* 22 (1):158.

349 Haas, B.J., A. Papanicolaou, M. Yassour, M. Grabherr, P.D. Blood *et al.*, 2013 De novo
350 transcript sequence reconstruction from RNA-seq using the Trinity platform for
351 reference generation and analysis. *Nat Protoc* 8 (8):1494-1512.

352 Haas, B.J., S.L. Salzberg, W. Zhu, M. Pertea, J.E. Allen *et al.*, 2008 Automated eukaryotic
353 gene structure annotation using EVidenceModeler and the Program to Assemble
354 Spliced Alignments. *Genome Biol* 9 (1):R7.

355 Harlow, P.S., and J.E. Taylor, 2000 Reproductive ecology of the jacky dragon
356 (*Amphibolurus muricatus*): an agamid lizard with temperature-dependent sex
357 determination. *Austral Ecology* 25 (6):640-652.

358 Henschel, R., M. Lieber, L.-S. Wu, P.M. Nista, B.J. Haas *et al.*, 2012 Trinity RNA-Seq
359 assembler performance optimization, pp. 45 in *Proceedings of the 1st Conference of
360 the Extreme Science and Engineering Discovery Environment: Bridging from the
361 eXtreme to the campus and beyond*. Association for Computing Machinery, Chicag,
362 IL, USA.

363 Hugall, A.F., R. Foster, M. Hutchinson, and M.S. Lee, 2008 Phylogeny of Australasian
364 agamid lizards based on nuclear and mitochondrial genes: implications for
365 morphological evolution and biogeography. *Biological Journal of the Linnean Society*
366 93 (2):343-358.

367 Kanehisa, M., and S. Goto, 2000 KEGG: Kyoto Encyclopedia of Genes and Genomes.
368 *Nucleic Acids Res* 28 (1):27-30.

369 Kent, W.J., 2002 BLAT--the BLAST-like alignment tool. *Genome Res* 12 (4):656-664.

370 Kim, D., J.M. Paggi, C. Park, C. Bennett, and S.L. Salzberg, 2019 Graph-based genome
371 alignment and genotyping with HISAT2 and HISAT-genotype. *Nat Biotechnol* 37
372 (8):907-915.

373 Kopylova, E., L. Noe, and H. Touzet, 2012 SortMeRNA: fast and accurate filtering of
374 ribosomal RNAs in metatranscriptomic data. *Bioinformatics* 28 (24):3211-3217.

375 Kumar, S., G. Stecher, M. Suleski, and S.B. Hedges, 2017 TimeTree: A Resource for
376 Timelines, Timetrees, and Divergence Times. *Mol Biol Evol* 34 (7):1812-1819.

377 Li, H., B. Handsaker, A. Wysoker, T. Fennell, J. Ruan *et al.*, 2009 The Sequence
378 Alignment/Map format and SAMtools. *Bioinformatics* 25 (16):2078-2079.

379 Lind, A.L., Y.Y.Y. Lai, Y. Mostovoy, A.K. Holloway, A. Iannucci *et al.*, 2019 Genome of
380 the Komodo dragon reveals adaptations in the cardiovascular and chemosensory
381 systems of monitor lizards. *Nat Ecol Evol* 3 (8):1241-1252.

382 Liu, Y., Q. Zhou, Y. Wang, L. Luo, J. Yang *et al.*, 2015 *Gekko japonicus* genome reveals
383 evolution of adhesive toe pads and tail regeneration. *Nat Commun* 6:10033.

384 Loytynoja, A., and N. Goldman, 2005 An algorithm for progressive multiple alignment of
385 sequences with insertions. *Proc Natl Acad Sci U S A* 102 (30):10557-10562.

386 Luo, R., B. Liu, Y. Xie, Z. Li, W. Huang *et al.*, 2012 SOAPdenovo2: an empirically
387 improved memory-efficient short-read de novo assembler. *Gigascience* 1 (1):18.

388 Majoros, W.H., M. Pertea, and S.L. Salzberg, 2004 TigrScan and GlimmerHMM: two open
389 source ab initio eukaryotic gene-finders. *Bioinformatics* 20 (16):2878-2879.

390 Margres, M.J., R.M. Rautsaw, J.L. Strickland, A.J. Mason, T.D. Schramer *et al.*, 2021 The
391 Tiger Rattlesnake genome reveals a complex genotype underlying a simple venom
392 phenotype. *Proc Natl Acad Sci U S A* 118 (4).

393 Minh, B.Q., H.A. Schmidt, O. Chernomor, D. Schrempf, M.D. Woodhams *et al.*, 2020 IQ-
394 TREE 2: New Models and Efficient Methods for Phylogenetic Inference in the
395 Genomic Era. *Mol Biol Evol* 37 (5):1530-1534.

396 Mitchell, A.L., T.K. Attwood, P.C. Babbitt, M. Blum, P. Bork *et al.*, 2019 InterPro in 2019:
397 improving coverage, classification and access to protein sequence annotations.
398 *Nucleic Acids Res* 47 (D1):D351-D360.

399 O'Leary, N.A., M.W. Wright, J.R. Brister, S. Ciufo, D. Haddad *et al.*, 2016 Reference
400 sequence (RefSeq) database at NCBI: current status, taxonomic expansion, and
401 functional annotation. *Nucleic Acids Res* 44 (D1):D733-745.

402 Oliver, P.M., and A.F. Hugall, 2017 Phylogenetic evidence for mid-Cenozoic turnover of a
403 diverse continental biota. *Nat Ecol Evol* 1 (12):1896-1902.

404 Pepper, M., M.D. Barquero, M.J. Whiting, and J.S. Keogh, 2014 A multi-locus molecular
405 phylogeny for Australia's iconic Jacky Dragon (Agamidae: *Amphibolurus muricatus*):
406 Phylogeographic structure along the Great Dividing Range of south-eastern Australia.
407 *Molecular Phylogenetics and Evolution* 71:149-156.

408 Peters, R.A., and C.S. Evans, 2003 Introductory tail-flick of the Jacky dragon visual display:
409 signal efficacy depends upon duration. *Journal of Experimental Biology* 206
410 (23):4293-4307.

411 Quast, C., E. Pruesse, P. Yilmaz, J. Gerken, T. Schweer *et al.*, 2013 The SILVA ribosomal
412 RNA gene database project: improved data processing and web-based tools. *Nucleic
413 Acids Res* 41 (Database issue):D590-596.

414 Roehr, J.T., C. Dieterich, and K. Reinert, 2017 Flexbar 3.0 - SIMD and multicore
415 parallelization. *Bioinformatics* 33 (18):2941-2942.

416 Smit, A.F., and R. Hubley, 2010 RepeatModeler Open-1.0. 2008-2015. Available at
417 <http://www.repeatmasker.org>.

418 Song, B., S. Cheng, Y. Sun, X. Zhong, J. Jin *et al.*, 2015a Anguidae lizard
419 (*Ophisaurusgracilis*) genome assembly data. *Dryad Digital Repository*. doi
420 10:100119.

421 Song, B., S. Cheng, Y. Sun, X. Zhong, J. Jin *et al.*, 2015b A genome draft of the legless
422 anguid lizard, *Ophisaurus gracilis*. *Gigascience* 4:17.

423 Stamatakis, A., 2006 RAxML-VI-HPC: maximum likelihood-based phylogenetic analyses
424 with thousands of taxa and mixed models. *Bioinformatics* 22 (21):2688-2690.

425 Stanke, M., O. Keller, I. Gunduz, A. Hayes, S. Waack *et al.*, 2006 AUGUSTUS: ab initio
426 prediction of alternative transcripts. *Nucleic Acids Res* 34 (Web Server issue):W435-
427 439.

428 Talavera, G., and J. Castresana, 2007 Improvement of phylogenies after removing divergent
429 and ambiguously aligned blocks from protein sequence alignments. *Syst Biol* 56
430 (4):564-577.

431 Tarailo-Graovac, M., and N. Chen, 2009 Using RepeatMasker to identify repetitive elements
432 in genomic sequences. *Curr Protoc Bioinformatics* Chapter 4:Unit 4 10.

433 Tian, R., H. Guo, C. Yang, G. Fan, S.L. Whiteley *et al.*, 2021 Assembled transcriptomes of
434 ovary, testis, and brain (male and female) of *Amphibolurus muricatus* (jacky dragon)
435 generated using Trinity v2.11.0, <https://doi.org/10.5281/zenodo.5523684>. Zenodo.

436 Tian, R., H. Guo, C. Yang, C. Shi, G. Fan *et al.*, 2023a Draft de novo genome assemblies of a
437 male and female *Amphibolurus muricatus* (jacky dragon),
438 <https://doi.org/10.5281/zenodo.8211053>. Zenodo.

439 Tian, R., H. Guo, C. Yang, C. Shi, G. Fan *et al.*, 2023b Gene annotations of *Amphibolurus
440 muricatus* (jacky dragon), *Intellagama lesueuri* (Australian water dragon),
441 *Phrynocephalus przewalskii* (Przewalski's toadhead agama), and *Phrynocephalus
442 vlangalii* (Ching Hai toadhead agama), <https://doi.org/10.5281/zenodo.8210940>.
443 Zenodo.

444 UniProt Consortium, 2012 Reorganizing the protein space at the Universal Protein Resource
445 (UniProt). *Nucleic Acids Res* 40 (Database issue):D71-75.

446 Wang, O., R. Chin, X. Cheng, M.K.Y. Wu, Q. Mao *et al.*, 2019 Efficient and unique
447 cobarcoding of second-generation sequencing reads from long DNA molecules
448 enabling cost-effective and accurate sequencing, haplotyping, and de novo assembly.
449 *Genome Res* 29 (5):798-808.

450 Warner, D., and R. Shine, 2008 The adaptive significance of temperature-dependent sex
451 determination in a reptile. *Nature* 451 (7178):566-568.

452 Warner, D.A., T. Uller, and R. Shine, 2013 Transgenerational sex determination: the
453 embryonic environment experienced by a male affects offspring sex ratio. *Scientific
454 reports* 3 (1):1-4.

455 Warren, R.L., C. Yang, B.P. Vandervalk, B. Behsaz, A. Lagman *et al.*, 2015 LINKS:
456 Scalable, alignment-free scaffolding of draft genomes with long reads. *Gigascience*
457 4:35.

458 Weisenfeld, N.I., V. Kumar, P. Shah, D.M. Church, and D.B. Jaffe, 2017 Direct
459 determination of diploid genome sequences. *Genome Res* 27 (5):757-767.

460 Whiteley, S.L., A. Georges, V. Weisbecker, L.E. Schwanz, and C.E. Holleley, 2021
461 Ovotestes suggest cryptic genetic influence in a reptile model for temperature-
462 dependent sex determination. *Proceedings of the Royal Society B* 288
463 (1943):20202819.

464 Woo, K., and G. Rieucau, 2013 Efficiency of aggressive and submissive visual displays
465 against environmental motion noise in Jacky dragon (*Amphibolurus muricatus*).
466 *Ethology Ecology & Evolution* 25 (1):82-94.

467 Xue, W., J.T. Li, Y.P. Zhu, G.Y. Hou, X.F. Kong *et al.*, 2013 L_RNA_scaffolder: scaffolding
468 genomes with transcripts. *BMC Genomics* 14:604.

469 Yang, Z., 2007 PAML 4: phylogenetic analysis by maximum likelihood. *Mol Biol Evol* 24
470 (8):1586-1591.

471 Zhu, B.H., J. Xiao, W. Xue, G.C. Xu, M.Y. Sun *et al.*, 2018 P_RNA_scaffolder: a fast and
472 accurate genome scaffolder using paired-end RNA-sequencing reads. *BMC Genomics*
473 19 (1):175.

474

475

476 **Figure legends**

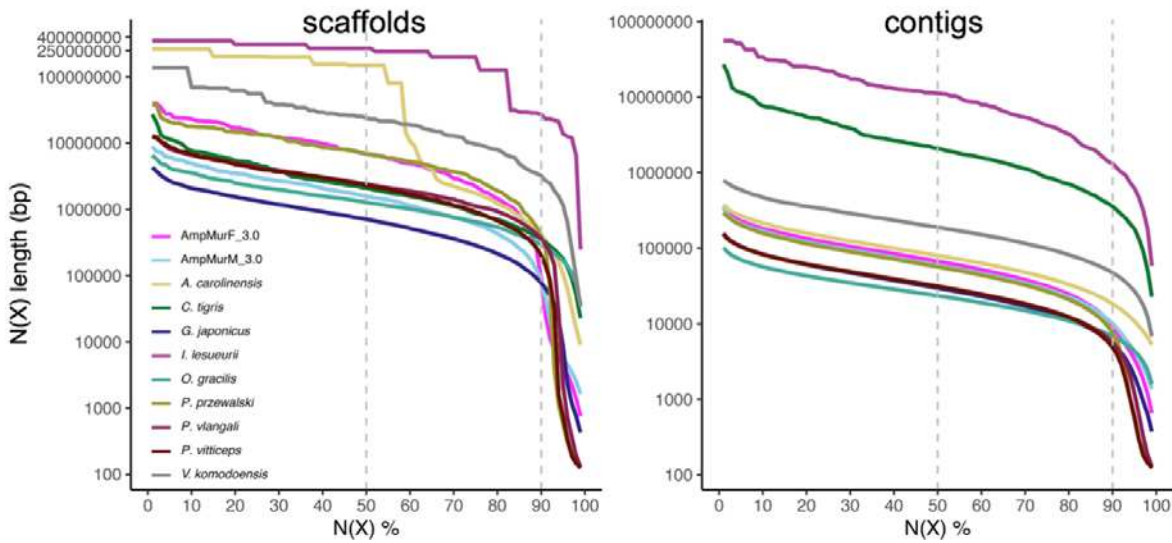


477

478 **Figure 1** Photograph of an adult male jacky dragon (*Amphibolurus muricatus*). Image credit:
479 David Cook Wildlife Photography.

480

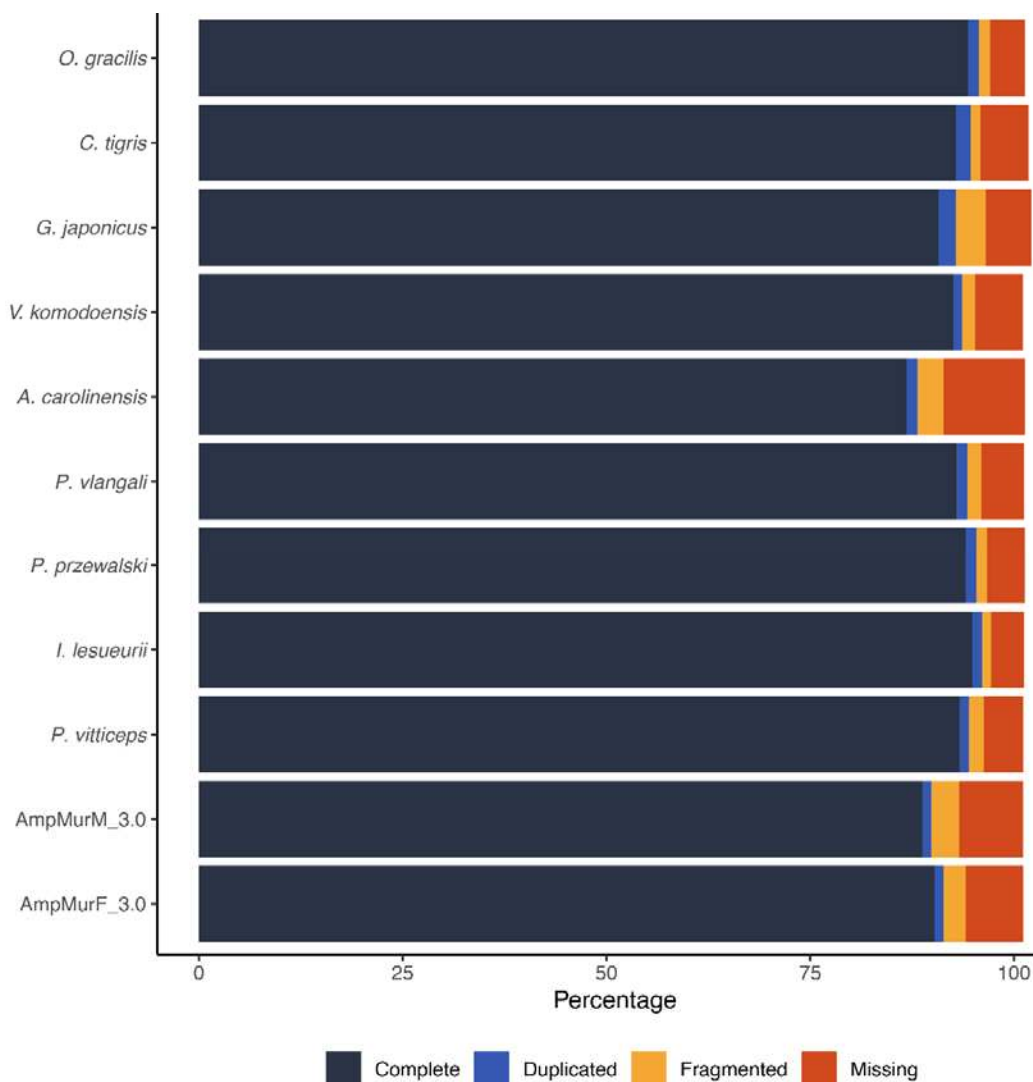
481



482

483 **Figure 2** Comparison of the contiguity of two *A. muricatus* assemblies and nine publicly
484 available squamate assemblies. N(x)% graphs show the (A) contig and (B) scaffold lengths
485 (y-axis), where x% (x-axis) of the genome assembly consist of scaffolds and contigs of at
486 least that size. Dashed, grey lines denote N50 and N90 values. AmpMurF_3.0 and
487 AmpMurM_3.0. denotes the female and male *A. muricatus* assembly, respectively
488

489



490

491 **Figure 3** BUSCO assessment of assemblies from ten squamate species. All genome
492 assemblies were examined using the same version and library of BUSCO (v5.0.0 with the
493 7,480-gene sauropsida_odb10 dataset). AmpMurF_3.0 and AmpMurM_3.0. denotes the
494 female and male *A. muricatus* assembly, respectively.

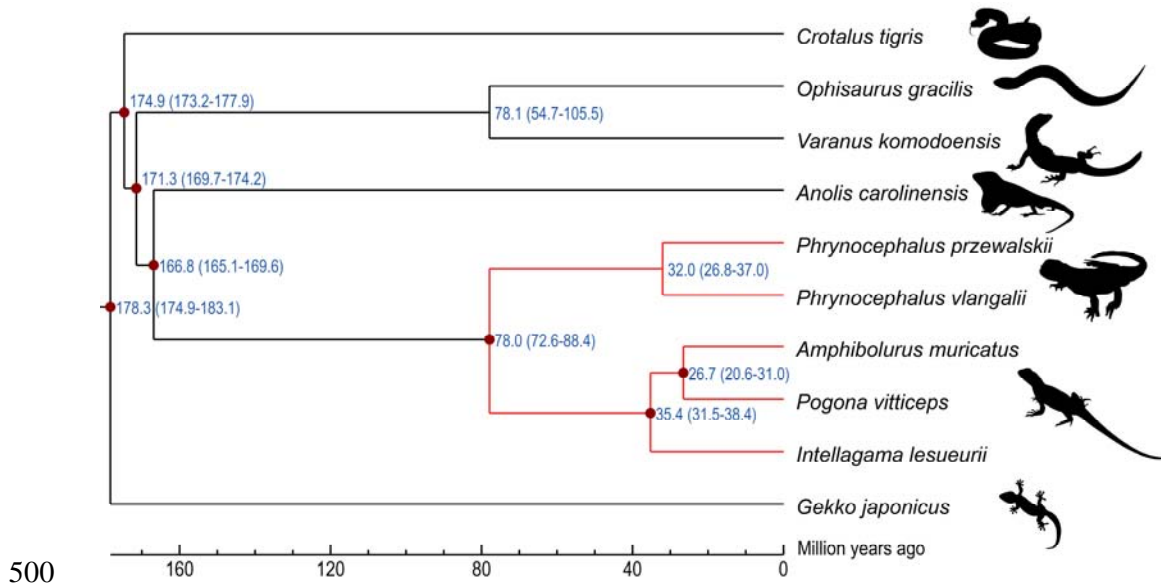
495

496

497

498

499



501 **Figure 4** Inferred phylogeny of ten squamate species based on whole-coding sequences of
502 4,441 1:1 orthologs. Numbers at nodes represent the estimated divergence time from present
503 (million years ago; Mya) between lineages. Agamid (family Agamidae) lineages are indicated
504 in red.

505
506
507

508 **Tables**

509 **Table 1 *A. muricatus* genome assembly statistics. Lengths in base pairs (bp).**

510 Note: assembly 1.0 denotes 10x Genomics Supernova; assembly 1.1, 10x Genomics Supernova + RNA read + Trinity scaffolding; assembly 2.0,
 511 10x Genomics Supernova (assembly 1.0) + SLR-superscaffolder (with stLFR reads); assembly 3.0, stLFR Supernova. Unmasked assemblies
 512 were interrogated.

Assembly methods	Female (AmpMurF_1.0)	Female (AmpMurF_1.1)	Female (AmpMurF_2.0)	Female (AmpMurF_3.0)	Male (AmpMurM_1.0)	Male (AmpMurM_1.1)	Male (AmpMurM_2.0)	Male (AmpMurM_3.0)
Contig number	154,897	124,200	154,961	145,095	180,498	151,787	180,576	95,472
Contig length	1,746,759,340	1,750,545,991	1,747,055,957	1,804,035,661	1,735,812,295	1,741,048,453	1,736,173,368	1,752,355,218
Contig N50 (bp)	25,056	37,220	25,053	67,166	21,019	28,761	21,019	59,294
Contig max length	209,568	348,284	209,568	645,479	196,238	288,200	196,238	773,372
Scaffold number	66,776	57,227	55,562	97,556	89,344	73,856	74,726	45,762
Scaffold length	1,840,499,790	1,841,491,868	1,871,715,150	1,868,109,324	1,831,120,515	1,833,283,242	1,854,210,455	1,804,786,947
Scaffold N50 (bp)	371,335	720,518	1,003,329	6,818,063	180,405	369,860	323,786	1,568,728
Scaffold max length	4,131,007	6,534,950	6,926,244	39,679,044	1,944,226	6,446,322	3,040,810	9,582,854
Gaps (bp)	93,740,450	90,945,877	124,659,193	64,073,663	95,308,220	92,234,789	118,037,087	52,431,729
Gaps (%)	5.09	4.94	6.66	3.43	5.20	5.03	6.37	2.91
GC content (%)	41.76	41.77	41.76	41.75	41.69	41.70	41.70	41.67

513



